Geophysical Research Letters

RESEARCH LETTER
10.1029/2023GL107310

**Key Points:**

- Transient simulations of the last deglaciation using GLAC1D and the new PaleoMist ice sheet reconstruction are compared for the first time
- AMOC stability is impacted by ice sheet reconstruction used and the combination of forcings, indicating its proximity to a bifurcation point
- PaleoMist simulation captures the BA/YD sequence signature in the northern North Atlantic

**Supporting Information:**

Supporting Information may be found in the online version of this article.

**Correspondence to:**

A. Masoum,
ahmadreza.masoum@awi.de

**Citation:**

Masoum, A., Nerger, L., Willeit, M., Ganopolski, A., & Lohmann, G. (2024). Lessons from transient simulations of the last deglaciation with CLIMBER-X: GLAC1d versus PaleoMist. *Geophysical Research Letters*, *51*, e2023GL107310. https://doi.org/10.1029/2023GL107310

Received 23 NOV 2023
Accepted 16 AUG 2024

**Author Contributions:**

**Conceptualization:** Ahmadreza Masoum, Lars Nerger, Gerrit Lohmann
**Data curation:** Ahmadreza Masoum
**Formal analysis:** Ahmadreza Masoum
**Investigation:** Ahmadreza Masoum
**Methodology:** Gerrit Lohmann
**Project administration:** Gerrit Lohmann
**Resources:** Gerrit Lohmann
**Software:** Matteo Willeit, Andrey Ganopolski
**Supervision:** Lars Nerger, Gerrit Lohmann
**Visualization:** Ahmadreza Masoum
**Writing – original draft:** Ahmadreza Masoum
**Writing – review & editing:** Lars Nerger, Matteo Willeit, Andrey Ganopolski, Gerrit Lohmann



# Lessons From Transient Simulations of the Last Deglaciation With CLIMBER-X: GLAC1D Versus PaleoMist

**Ahmadreza Masoum[1,2], Lars Nerger[1], Matteo Willeit[3], Andrey Ganopolski[3], and Gerrit Lohmann[1,2]**

[1]Alfred Wegener Institute, Helmholtz Centre for Polar and Marine Research, Bremerhaven, Germany, [2]Center for Marine Environmental Sciences, University of Bremen, Bremen, Germany, [3]Potsdam Institute for Climate Impact Research, Potsdam, Germany

**Abstract** The last deglaciation experienced the retreat of massive ice sheets and a transition from the cold Last Glacial Maximum to the warmer Holocene. Key simulation challenges for this period include the timing and extent of ice sheet decay and meltwater input into the oceans. Here, major uncertainties and forcing factors for the last deglaciation are evaluated. Two sets of transient simulations are performed based on the novel ice-sheet reconstruction PaleoMist and the more established GLAC1D. The simulations reveal that the proximity of the Atlantic meridional overturning circulation (AMOC) to a bifurcation point, where it can switch between on- and off-modes, is primarily determined by the interplay of greenhouse gas concentrations, orbital forcing and freshwater forcing. The PaleoMist simulation qualitatively replicates the Bølling-Allerød (BA)/Younger Dryas (YD) sequence: a warming in Greenland and Antarctica during the BA, followed by a cooling northern North Atlantic and an Antarctic warming during the YD.

**Plain Language Summary** The last deglaciation, spanning roughly 20,000 to 10,000 years ago, marked a period of Earth's history characterized by the retreat of massive ice sheets that had covered large parts of the planet. During this phase, a drastic transition occurred from the cold Last Glacial Maximum to the warmer and more stable climate of the Holocene. A main challenge for simulating the last deglaciation is the timing and amplitude of the ice sheet decay and the amount of meltwater that enters into the oceans. Using two different reconstructions of ice sheets, we employ an efficient climate model to explore changes at the end of the last ice age. Our comparison shows notable differences in the timing and amplitude of abrupt climate events in the simulations using two different ice-sheet reconstructions. Furthermore, we investigate the effects of factors such as greenhouse gases and Earth's orbital changes on the large-scale ocean currents with respect to underlying ice sheets. Ultimately, our study sheds light on how different elements of the Earth's system shape the termination of the last ice age, enriching our understanding of Earth's climate history and guiding further deglaciation scenarios.

## 1. Introduction

During the last deglaciation, 20-10 kyr before the present (BP), all climate variables encountered large-scale changes. From a cold Last Glacial Maximum (LGM), the climate state transited to the warm interglacial state. This transition was triggered by changes in insolation and geochemical processes (Paillard, 2015). Furthermore, greenhouse gas (GHG) concentrations rose by 80–100 ppm (Monnin et al., 2001; Spahni et al., 2005; Veres et al., 2013) and ice sheets melted, and positive feedbacks occurred (Clark et al., 2012). As a result, the atmospheric and oceanic circulation experienced significant changes (e.g., Löfverström & Lora, 2017; Pöppelmeier et al., 2023), and the global mean sea level rose by about 100–130 m (e.g., Gowan et al., 2021; Lambeck et al., 2014). However, these changes did not happen steadily; some abrupt events, pronounced in Greenland ice records, such as the warming during the Bølling-Allerød (BA; Clark et al., 2002; Weaver et al., 2003) or the cooling during the Younger Dryas (YD; Carlson et al., 2007) occurred during the last deglaciation.

Modellers are striving to simulate the last deglaciation to improve our understanding of climate change mechanisms and enhance model accuracy. Accurate simulations allow scientists to refine their models, leading to better future climate predictions. This period's major changes in ice sheets, ocean circulation, and $CO_2$ levels are crucial for understanding the climate system. Insights from these simulations inform Earth's climate sensitivity, regional responses, and strategies for mitigating climate change effects. Several studies highlight different facets of glacial-interglacial climate, including the last deglaciation, by employing model simulations with prescribed ice sheet changes (e.g., He, 2011; Knorr & Lohmann, 2007; Liu et al., 2009; Sun et al., 2022; Zhang et al., 2014b, 2017) or more complicated simulations done by coupled ice sheet-climate modeling (e.g., Abe-Ouchi et al., 2013; Ganopolski & Calov, 2011; Gregoire et al., 2015). Ganopolski and Calov (2011) and Abe-Ouchi et al. (2013) emphasized that orbital changes primarily drive glacial-interglacial cycles. Zhang et al. (2021) showed that an abrupt transition from warm interstadial to cold stadial states could be initiated directly by precession and obliquity changes. Gregoire et al. (2015) suggested that orbital forcing is the main driver of the reduction of North American ice sheets, while GHG forcing accounts for 30% contribution as the second driver. GHG, particularly $CO_2$, are essential for the amplitude of the cycles and result in complete deglaciation (Abe-Ouchi et al., 2013; Charbit et al., 2005; Ganopolski & Calov, 2011; Heinemann et al., 2014). Prescribing ICE-4G ice sheets (W. R. Peltier, 1994), Timmermann et al. (2009) indicated that orbital forcing and atmospheric $CO_2$ increase initiate the warming around Antarctica without direct triggers from the Northern Hemisphere.

Previous studies showed that a primary source of uncertainty in the glacial-interglacial simulations is the ice sheet evolution, which has a decisive influence on the timing and occurrence of climate events (e.g., Bakker et al., 2020; Kapsch et al., 2022; Ullman et al., 2014; Zhang et al., 2014b). Ice sheet heights are important for simulating the atmospheric (Kageyama & Valdes, 2000; Löfverström et al., 2014) and oceanic circulation (Sherriff-Tadano et al., 2018; Zhang et al., 2014b; Zhu et al., 2014). Kapsch et al. (2022) and Bouttes et al. (2023) follow the protocol of the Intercomparison Project Phase four (PMIP4; Kageyama et al., 2017) for transient simulation of the last deglaciation (Ivanovic et al., 2016), and compare the effect of the ICE-6G (Argus et al., 2014; W. R. Peltier et al., 2015) and GLAC1D (Briggs et al., 2014; Tarasov et al., 2012) ice sheet reconstructions. Consistent with the control of the ocean circulation by ice sheet height (Zhang et al., 2014b), Kapsch et al. (2022) indicate that topography differences lead to changes in the jet stream's magnitude, the atmospheric circulation, and river directions in the last deglaciation. Bouttes et al. (2023) employ an Earth system model of intermediate complexity (EMIC) and show that changes in bathymetry lead to a cooling in the deglaciation simulations. In addition, the use of evolving ice sheets implies changes in freshwater flux into the ocean, affecting the Atlantic meridional overturning circulation (AMOC) (Kageyama et al., 2010; McManus et al., 2004; Stouffer et al., 2007). The deglacial AMOC strongly depends on the timing and magnitude of freshwater forcing at high latitudes of the North Atlantic or Arctic, where deep water forms (e.g., Lohmann et al., 2020; Roche et al., 2010; Smith & Gregory, 2009; Stouffer et al., 2006). When the freshwater shifts over a critical value, called bifurcation point (Held & Kleinen, 2004), the AMOC can shift or fluctuate between modes (e.g., Kapsch et al., 2022; Klockmann et al., 2018; Lohmann & Schneider, 1999; Sun et al., 2022; Zhang et al., 2017). Accordingly, AMOC instability can lead to abrupt climate changes during the last deglaciation (e.g., Clark et al., 2002; Knorr & Lohmann, 2007; Lohmann & Schulz, 2000). Bethke et al. (2012) conduct sensitivity simulations with the ICE-5G (W. R. W. R. Peltier, 2004) reconstruction and investigate different combinations of GHG, orbital, and ice sheet forcing. They suggest that ice sheet reconstructions provide limited constraints on the timing, volume, and location of the freshwater discharges associated with melting ice sheets.

Due to uncertainty in ice-sheet evolution and the meltwater derived from them, transient simulations of the last deglaciation (e.g., Bouttes et al., 2023; Kapsch et al., 2022; Liu et al., 2014) show discrepancies in terms of global mean surface temperature (GMST) and AMOC strength compared to the proxy-based reconstructions (e.g., Marcott et al., 2013; McManus et al., 2004; Osman et al., 2021; Shakun et al., 2012), particularly during the BA and YD. Hence, the PMIP4 protocol prescribes two reconstructions, GLAC1D and ICE-6G, as boundary conditions for ice-sheet evolution. However, the freshwater derived from these reconstructions is not sufficiently accurate to replicate GMST and AMOC comparable to the proxies (e.g., Bouttes et al., 2023). These reconstructions are calculated by inverse modeling and exhibit notable uncertainties, attributed mainly to the viscosity model employed for the solid Earth. This paper presents transient simulations of the last deglaciation with an EMIC, CLIMBER-X (Willeit et al., 2022). EMICs are well-suited for long-term climate system integrations (Claussen et al., 2002) and are capable of simulating deglaciation (Bonelli et al., 2009; Charbit et al., 2005; Ganopolski & Calov, 2011; Heinemann et al., 2014). To address the uncertainty caused by ice-sheet reconstruction, we employ a new ice-sheet reconstruction, PaleoMist (Gowan et al., 2021), that is used for the first time as an ice-sheet boundary condition for the last deglaciation. PaleoMist reconstructs the ice sheets using different methodologies and prescribes the different freshwater schemes in the last deglaciation simulation. We primarily aim to evaluate the deglacial climate as simulated by CLIMBER-X with PaleoMist by comparing it with the GLAC1D simulation. Moreover, we examine the role of the other two forcings prescribed by the PMIP4 protocol, GHG and orbital, during the last termination with respect to the underlying ice sheets and by isolating the effects of orbital, GHG, and ice sheets.

## 2. Method

### 2.1. Model

CLIMBER-X, the version of Willeit et al. (2022), employs several sub-models to simulate various climate components. It employs the semi-empirical statistical–dynamical atmosphere model (SESAM; Willeit et al., 2022), the 3-D frictional–geostrophic ocean model GOLDSTEIN (N. R. Edwards et al., 1998; N. Edwards & Shepherd, 2002; N. R. Edwards & Marsh, 2005), the thermodynamic sea ice model (SISIM; Willeit et al., 2022), and the land surface model PALADYN (Willeit & Ganopolski, 2016). CLIMBER-X's horizontal resolution is set to $5° \times 5°$ for all components. The model is designed to capture the mean climatological state and can simulate at a speed approximately 100–1,000 times faster than full general circulation models when using comparable computational resources (Willeit et al., 2022).

### 2.2. Choice of Ice Sheet Reconstruction

PaleoMist and GLAC1D use different methodologies to reconstruct the past ice sheets. GLAC1D creates the Greenland Ice Sheet based on an ice sheet modeling exercise that was tuned to fit Holocene sea level observations (Tarasov & Richard Peltier, 2002). Antarctica and North American ice sheets are based on an ensemble average of several thousand ice sheet model simulations that scored favorably in fitting constraints such as Holocene sea level changes and present-day uplift rates (Briggs et al., 2014; Tarasov et al., 2012). Conversely, PaleoMist calculates the ice sheet using the ICESHEET program (Gowan et al., 2016), which assumes perfectly plastic, steady-state conditions for the ice sheet (i.e., the lateral shear stresses are ignored, and the ice surface is not dynamically changing). Employing the model SELEN (Spada & Stocchi, 2007), changes in sea level and Earth's deformation are computed using a time series of ice sheet changes. Finally, the sea level change is added to modern topography and the ice sheet thickness to produce a paleo-topography reconstruction (Gowan et al., 2021). Due to the above differences, the sea level increases linearly in PaleoMist while showing variation in GLAC1D, particularly during BA and YD (see Figure S1 in Supporting Information S1).

While the differences in methodologies between PaleoMist and GLAC1D are significant, it is essential to address the criticisms and responses surrounding PaleoMist as a novel reconstruction to understand their broader implications fully. Yokoyama et al. (2022) criticize that PaleoMist is based only on near-field constraints, resulting in discrepancy with previous studies (e.g., Clark & Tarasov, 2014) in the estimation of the relative sea level. To reply to Yokoyama et al. (2022), Gowan et al. (2022) reason that by relying on near-field constraints, PaleoMist would be independent of deep-sea foraminifera and avoid sea-level proxies with high uncertainties. Moreover, Gowan et al. (2022) question in using spherically symmetric Earth structures to represent far-field sea level. Therefore, Gowan et al. (2021) utilize non-ice sheet proxies not as absolute constraints but to test PaleoMist qualitatively. This debate highlights the complexities and potential uncertainties in ice sheet reconstruction methodologies, underscoring the need for a cautious interpretation of sea-level data and the importance of considering multiple approaches for a comprehensive understanding of ice sheet roles in the simulation of the last deglaciation.

### 2.3. Experimental Design

We conduct two sets of transient deglaciation simulations, Exp_GLAC1D and Exp_PaleoMist, each consisting of five simulations: full-forced (GLAC1D_full and PaleoMist_full), with constant ice sheet reconstruction (GLAC1D_fixIce and PaleoMist_fixIce), with constant GHG (GLAC1D_fixGHG and PaleoMist_fixGHG), with constant orbital forcing (GLAC1D_fixOrbit and PaleoMist_fixOrbit), and pre-industrial (PI) simulation (GLAC1D_PI and PaleoMist_PI; Table S1 in Supporting Information S1). In both experiments, GHG concentrations and orbital parameters are prescribed by Köhler et al. (2017) and Laskar et al. (2004), respectively. In addition, the GLAC1D reconstruction (Briggs et al., 2014; Tarasov et al., 2012; Tarasov & Richard Peltier, 2002) is used for ice sheets, bathymetry, and land-sea mask in Exp_GLAC1D, while Exp_PaleoMist employs the PaleoMist reconstruction (Gowan et al., 2021). Except for PI simulations, full-forced simulations are integrated from 25 kyr BP with pre-industrial equilibrium and then switch to LGM boundary conditions. The model is subsequently run until the year 6.5 kyr BP. We prescribe time-varying topography, bathymetry, greenhouse gases

(GHG; $CO_2$, $N_2O$, $CH_4$), and orbital parameters into the full-forced simulations. The GHG and orbital parameters forcing field is updated yearly, while topography, bathymetry, and ice sheet distribution are changed every 100 years. In the model, the freshwater (FW) flux to the ocean is computed from a combination of precipitation-evaporation, sea ice fluxes, and land runoff. Additionally, the prescribed changes in ice thickness are converted into a liquid water flux that is routed into the ocean following the steepest surface gradient.

The sensitivity simulations begin with boundary conditions from 22 kyrs BP, and throughout the simulation, the corresponding forcing remains constant at the 22 kyrs BP level, while the other forcing factors vary over time. We prescribe the LGM values recommended in the PMIP4 protocol (Kageyama et al., 2017). This means that in simulations with constant GHG forcing, $CO_2$, $N_2O$, and $CH_4$ were set to 190 ppm, 200 ppb, and 375 ppb, respectively. Similarly, eccentricity, obliquity, and perihelion are kept constant in simulations with constant orbital forcing at 0.018994, 22.949°, and 114.42°, respectively. This configuration is intentionally designed to determine the distinct role of individual forcing factors. Finally, we define PI as the year 1850 and follow PMIP4 instructions for applying GHG and orbital forcings in the PI simulations.

## 3. Results and Discussion

### 3.1. Sensitivity Simulations to Different Forcings

In Figure 1, the left panels show the deglacial dynamics for Exp_GLAC1D, whereas the right panels are for Exp_PaleoMist. We perform sensitivity forcing experiments, maintaining different deglacial forcing components at LGM levels. In scenarios with fixed ice sheets and bathymetry (blue lines in Figure 1), North Atlantic FW forcing (≥30° N, including freshwater in the Arctic Ocean) remains near LGM levels. Consequently, North Atlantic SSS and AMOC show minor changes. However, in Exp_GLAC1D, FW forcing slightly exceeds Exp_PaleoMist in average by approximately 0.05 Sv, resulting in a weaker early Holocene AMOC. GLAC1D_fixIce and PaleoMist_fixIce simulations underestimate the last deglaciation warming, yielding an early Holocene GMST approximately 2.5°C warmer than LGM. This result aligns with the anticipated consequences of constant FW forcing and albedo effects. Furthermore, these simulations do not replicate the abrupt events during the last deglaciation, possibly due to constant ice sheet heights during the simulations. Zhang et al. (2014a) indicate that changes in northern hemisphere ice sheet height can trigger rapid climate shifts.

In simulations with constant GHG forcing (red lines in Figure 1), FW forcing is higher than in full-forced simulations due to more precipitation occurring in the fixGHG simulations (see Figures S2, S3, and S4 in Supporting Information S1). This is notable in Exp_PaleoMist during YD and early Holocene (Figure 1b). When FW exceeds approximately 0.24 Sv during the simulations, AMOC transitions to off-mode. This transition aligns with HS1 culmination in Exp_GLAC1D (Figure 1e) and YD onset in Exp_PaleoMist (Figure 1f). This supports Zhang et al. (2017) results, suggesting atmospheric $CO_2$ changes critically impact the timing of AMOC transitions. Nonetheless, abrupt declines in FW within GLAC1D_fixGHG lead to sudden AMOC strengthening, subsequently resulting in a rapid increase in GMST. Furthermore, the GMST increases only by approximately 3°C during deglaciation in simulations featuring constant GHG forcing. This underscores the significant role played by transient GHG concentrations in driving the last deglaciation process.

There is a conspicuous FW forcing in GLAC1D_fixOrbit and PaleoMist_fixOrbit (green lines in Figure 1). Ice sheets' contribution to FW forcing remains unchanged across full-forced, constant GHG and orbital simulations. However, there are substantial variations in precipitation patterns, global mean precipitation, and evaporation between these simulations and the full-forced ones (see Figures S2, S3, and S4 in Supporting Information S1).

GLAC1D_fixOrbit and PaleoMist_fixOrbit depict higher precipitation in the Northern Hemisphere, leading to increased FW in the North Atlantic. Furthermore, AMOC transitions to an off-mode state at comparable times (as shown in Figures 1e and 1f) as in simulations with constant GHG forcing. This finding aligns with the outcomes of a study by Zhang et al. (2021), which demonstrated that precession and obliquity play influential roles in shaping hydroclimate in glacial-interglacial cycles. GHG and orbital forcings influence FW fluxes by changing precipitation patterns, with a sustaining effect on the AMOC. Moreover, the GLAC1D_fixOrbit and PaleoMist_fixOrbit simulations effectively replicate the increase of approximately 5°C in GMST during the last deglaciation. This underscores the significant impact of GHG and ice sheets on the simulation of global temperatures during this period, although such forcing also affects the dynamics of AMOC.

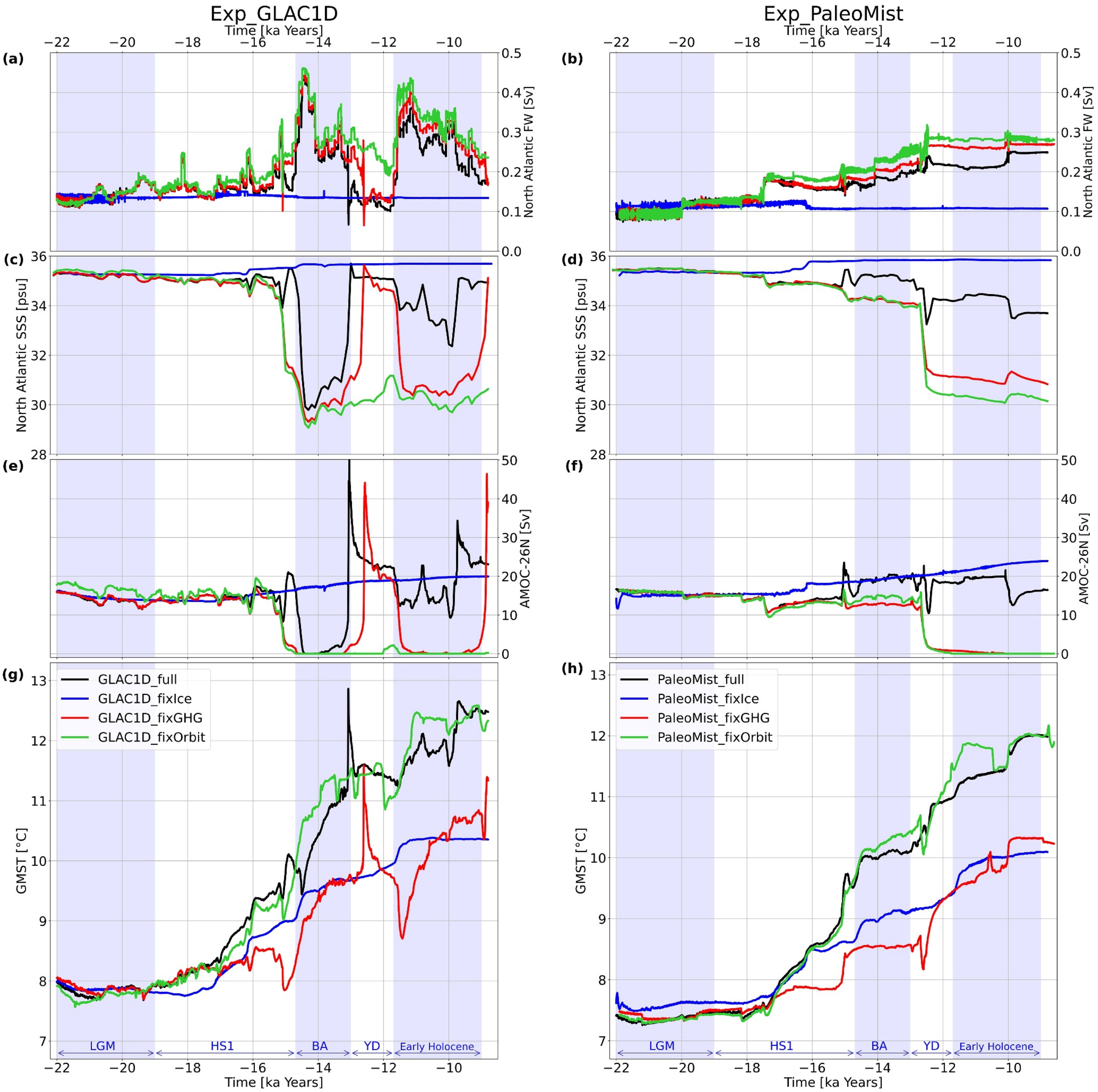


**Figure 1.** North Atlantic FW, North Atlantic SSS, AMOC at 26°N, and GMST for Exp_GLAC1D (a),(c),(e),(g), and for Exp_PaleoMist (b),(d),(f), and (h). We define LGM as 22–19 kyr BP, Heinrich Stadial 1 (HS1) as 19–14.7 kyr BP, BA as 14.7–13 kyr BP, and YD as 13–11.6 kyr BP. North Atlantic index for SSS is defined as an average over 50°N–70°N and 45°W–0°W. The blue background represents LGM, BA, and early Holocene, while the white background represents HS1 and YD. Note that the vertical axes differ for Exp_GLAC1D and Exp_Paleomist except for GMST panels (g) and (h). North Atlantic FW flux encompasses precipitation-evaporation, sea ice fluxes, land runoff, and liquid water flux melted from ice sheets.

### 3.2. Full-Forced Simulations: GLAC1D Versus PaleoMist

After analyzing the effects of different forcing mechanisms individually in the previous subsection, we now proceed to evaluate the climate during the last deglaciation. In this subsection, we compare the GLAC1D simulation with the PaleoMist simulation to understand the differences and similarities between these simulations and the implications of ice sheet choice in modeling the deglaciation climate. In full-forced simulations (black lines in Figure 1), North Atlantic SSS (Figures 1c and 1d) is anti-correlated with North Atlantic FW forcing

(Figures 1a and 1b) and reduced by about one psu during the simulations. This reduction is attributable to the freshwater contributions resulting from ice sheet melting (Broecker, 2002; Clark et al., 2012). North Atlantic SSS differs from 1 to 5 psu between GLAC1D_full and PaleoMist_full during various temporal segments (Figures 1c and 1d). GLAC1D_full is less saline over the Atlantic and more saline at the surface of the other oceans (see Figure S5 in Supporting Information S1). During BA, due to the shutdown of AMOC in Exp_GLAC1D (Figure 1e), the northward transport of warm and saline water is disrupted, producing pronounced differences (exceeding 5 psu in North Atlantic) relative to Exp_PaleoMist (Figures 1c and 1d). During YD, GLAC1D_full simulates more saline surface water near Greenland, where deep water forms in the North Atlantic (Figures 1c and 1d). This phenomenon is potentially linked to the stronger AMOC in GLAC1D_full compared to PaleoMist_full (Figures 1e and 1f).

The glacial sea surface temperature anomaly (ΔSST) relative to PI period is almost identical over the northern hemisphere in GLAC1D_full and PaleoMist_full (see Figure S7 in Supporting Information S1). The global ΔSST during LGM (average over 22-19 kyr BP) is −2.18 and −2.15°C for GLAC1D_full and PaleoMist_full, respectively. These results are around 1°C warmer than cooling 3.14 ± 0.29°C reconstructed by Tierney et al. (2020). During the Northern Hemisphere winter, PaleoMist_full and GLAC1D_full are consistent with MARGO (MARGO, 2009) over the Southern Ocean western Atlantic. In the Southern Ocean eastern Atlantic, PaleoMist_full shows more cooling than GLAC1D_full and aligns better with MARGO. However, in the Southern Ocean western Pacific, MARGO indicates colder temperatures than our simulations (Table S2 in Supporting Information S1).

The simulated global cooling during the LGM (average over interval 22–19 ka BP), relative to PI, amounts to 6.12°C in PaleoMist_full and 5.9°C in GLAC1D_full. These results are in agreement with the data assimilation-based estimate of 6.05 ± 0.43°C by Tierney et al. (2020), the data assimilation-based estimate of 6.75 ± 0.48°C by Osman et al. (2021), and the model-based estimate of 6.2°C in Willeit et al. (2022). However, Annan et al. (2022) reconstructed a smaller GMST anomaly (LGM-PI) of 4.5 ± 0.9°C. PaleoMist_full depicts a colder LGM GMST (by approximately 0.5°C) than GLAC1D_full due to higher ice sheet altitudes. This 0.5°C difference is more than the difference between the 6.12 and 5.9°C anomalies because of the difference in GLAC1D_PI and PaleoMist_PI temperatures.

Snoll et al. (2024), a multi-model intercomparison study of the early part of the last deglaciation (20–15 ka BP), show that strong AMOC leads to regional warming in Greenland and the North Atlantic. At the same time, disruptions due to meltwater input can cause significant cooling. The AMOC state at the end of LGM is significant in determining the sensitivity of models to FW forcing during HS1. Models with a stronger and deeper AMOC are less sensitive to FW inputs compared to those with a weaker and shallower AMOC. In alignment with Snoll et al. (2024), GLAC1D_full and PaleoMist_full show warming by 15 ka BP and a strong correlation between GMST and AMOC (Figures 1g and 1h).

During BA, GLAC1D_full oceans are warmer than PI in most regions (see Figure S7 in Supporting Information S1) due to an abrupt AMOC shift (Figure 1e), leading to an abrupt increased temperature at the end of BA. The main differences between full forced simulations occur during BA due to significant FW flux differences (see Figure S8 in Supporting Information S1) and very different AMOC (Figures 1e and 1f). GLAC1D includes significant ice volume loss during BA in the North Atlantic, associated with the major meltwater pulse MWP-1A (W. Peltier, 2005), resulting in substantial FW influx (Figure 1a). GLAC1D loses $0.225 \times 10^7$ $km^3$ ice more than PaleoMist during BA. This configuration imparts a diminished AMOC in GLAC1D_full (Figure 1e), correspondingly inducing lower SSS in the North Atlantic relative to PaleoMist_full.

The AMOC alterations are often proposed as a main factor in abrupt climate shifts during the last deglaciation (e.g., Clark et al., 2002; Knorr & Lohmann, 2007; Lohmann & Schulz, 2000; Snoll et al., 2024). AMOC strengthening during the BA compared to HS1 is observed in reconstructions (McManus et al., 2004; Ng et al., 2018) and modeling studies (e.g., Liu et al., 2009). In GLAC1D_full, AMOC increases at the end of HS1 but experiences an off-mode transition at the onset of the BA period, followed by a substantial resurgence at the end of the BA (Figure 1e). The sudden reduction in AMOC during BA is common in the transient simulations prescribing GLAC1D (e.g., Broecker, 2002; Clark et al., 2012) (see Figure S9 in Supporting Information S1). In PaleoMist_full, AMOC has an abrupt increase and reduction at the end of HS1. It increases considerably at the onset of BA and is almost stable by the end of BA (Figure 1f). In both simulations, the abrupt strengthening of AMOC occurs before BA. As shown in Figure 1 for different simulations, the timing of the abrupt changes in the

AMOC depends on the FW flux. Obase and Abe-Ouchi (2019) suggested that the gradual increase in atmospheric $CO_2$ during HS1 may cause a weakening of stratification of the North Atlantic, which results in an abrupt rise in the AMOC during the BA transition. In contrast to BA, McManus et al. (2004) indicated AMOC was weak during YD. In GLAC1D_full, AMOC after the overshoot decreases gradually during YD, while in PaleoMist_full, it experiences variations and an abrupt reduction (Figures 1e and 1f). Furthermore, a YD-like event for AMOC is observed in PaleoMist_full in the early Holocene at 10 ka BP due to an increase in FW influx. This maximum FW occurs in the early Holocene because of the time resolution of the PaleoMist reconstruction, which is 2,500 years. At 10 ka BP, ice sheets suddenly decrease, resulting in the North Atlantic FW growth.

When comparing the evolution of North Atlantic SST in the simulations with a corresponding marine climate record (Shakun et al., 2012), PaleoMist_full simulation reflects the warming and cooling patterns over the North Atlantic during BA and YD periods. In contrast, the GLAC1D_full simulation suggests cooling during the BA, followed by a sudden increase and decrease, and relatively stable temperature during YD (Figures 2a–2c).

For the BA/YD sequence in GMST, the Shakun and Osman reconstructions show a "warming-cooling-warming" sequence in global mean surface temperature (GMST; Figure 2d). In GLAC1D_full, the transition from BA to YD is also seen, following AMOC pattern (Figures 1e and 1g). If the abrupt reduction and overshoot during BA are ignored, GLAC1D_full shows a "warming-cooling-warming" sequence, but this sequence is late with respect to the reconstructions (Figure 2d). Moreover, the warming of the BA in GLAC1D_full matches neither NGRIP nor DomeC temperature records (Figures 2a and 2b). Comparing Buttes_GLAC1D and GLAC1D_full, AMOC shifts to the weak mode simultaneously at the onset of BA in both simulations. Still, the timing and magnitude of overshoot of AMOC at the onset of YD is mostly a model-dependent feature, and consequently, the GMST trajectory is different in GLAC1D_full (see Figure S9 in Supporting Information S1).

Conversely, GMST within the PaleoMist_full scenario follows mainly GHGs (Figure 1h), with some shorter variations (≈0.25°C) at the onset of the BA (warming-cooling-warming) occurred much earlier than reconstructions (Figure 2d). Moreover, there is a minor short-term cooling (≈0.1°C) during the YD, which is not comparable with the reconstruction cooling. Generally, a "warming-stable-warming" sequence from −15 to −12.5°kyr BP is observed in PaleoMist_full for GMST and temperatures in DomeC and NGRIP locations (Figures 2b and 2d).

Finally, Figures 3d–3g indicate surface temperature anomalies between the BA and HS1 and between YD and BA for both PaleoMist_full and GLAC1D_full. PaleoMist_full shows a pronounced warming between the BA and HS1 and a moderate cooling between YD and BA in the northern North Atlantic. The opposite is found for GLAC1D_full with cooling between the BA and HS1 and warming between YD and BA. The deglacial meltwater and its influence on AMOC affect the timing of the two-step character "cold-warm-cold-warm" during the termination: For PaleoMist_full, the HS1-stadial comes along with a weaker AMOC and a stronger AMOC during BA (Figures 3a and 3b), in contrast to GLAC1D_full. The PaleoMist simulations replicate, at least qualitatively, the BA/YD sequence with respect to reconstructions: a warming in Greenland and Antarctica in the BA, a cooling northern North Atlantic, and a warming in Antarctica in the YD.

## 4. Conclusions

This study pioneers the use of the PaleoMist ice sheet reconstruction (Gowan et al., 2021) to simulate the last deglaciation, contrasted with the more traditional GLAC1D reconstruction (Briggs et al., 2014; Tarasov et al., 2012). In both PaleoMist and GLAC1D simulations, LGM temperatures and southern ocean Atlantic SSTs are consistent with data assimilation-based estimates of Tierney et al. (2020) and MARGO (2009), respectively.

Variations in sea level pressure, wind patterns, and surface temperatures, especially during the BA warm period, illustrate the different behavior of GLAC1D and PaleoMist. These differences are attributed to the varying configurations, extents, and topographies of the ice sheets, affecting the atmosphere-ocean circulation. We show that the PaleoMist simulation outperforms GLAC1D in capturing the pronounced warming in the northern North Atlantic, which is a main characteristic of BA (Buizert et al., 2014). In agreement with previous studies (e.g., Bethke et al., 2012; Bouttes et al., 2023; Kapsch et al., 2022), we find that the timing and magnitude of climate events during the termination are affected by the ice sheet reconstruction. PaleoMist shows greater glacial ice sheet heights, particularly in the Northern Hemisphere, while GLAC1D has a substantial ice sheet volume loss, causing an off-mode in the AMOC during the BA. The strong fluctuations in deglacial meltwater in GLAC1D

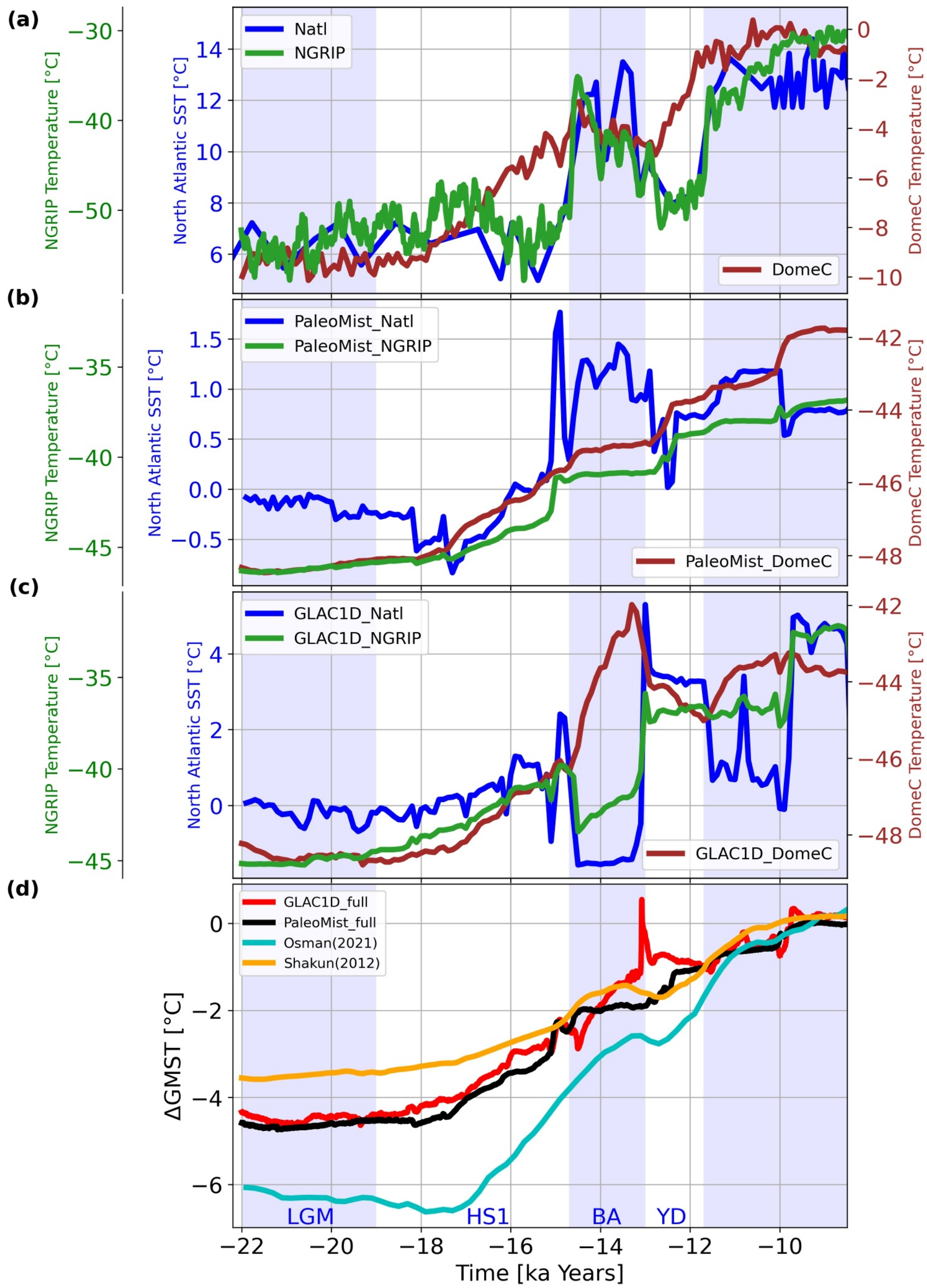


**Figure 2.** (a) Evolution of temperature at NGRIP (Greenland), DomeC (Antarctica), and SST at North Atlantic (NA87-22; Waelbroeck et al., 2001), (b) Evolution of temperature at NGRIP, DomeC, and SST at North Atlantic in PaleoMist_full, (c) Evolution of temperature at NGRIP, DomeC, and SST at North Atlantic in GLAC1D_full, and (d) GMST anomaly from the early Holocene (defined as 11.5–6.5 ka BP) for GLAC1D_full, PaleoMist_full, Shakun et al. (2012), and Osman et al. (2021). Data for NGRIP, DomeC, and NA87-22 in (a) are from Shakun et al. (2012). North Atlantic index for SST in (b) and (c) is defined as an average over 50°N–70°N and 45°W–0°W. Discrepancies between Shakun et al. (2012) and Osman et al. (2021) reconstructions are due to utilizing different observation data sets, background states, and methods. Note that there are different vertical axes for different variables.

lead to abrupt changes in global mean temperature and fail to capture the BA/YD transition sequence. The freshwater derived from PaleoMist does not induce an off-mode AMOC during the BA but a pronounced warming in the North Atlantic realm. The YD cooling in the PaleoMist simulation seems to be underestimated for this area, especially over Greenland, where most likely a pronounced overshoot dynamics is relevant (Knorr &

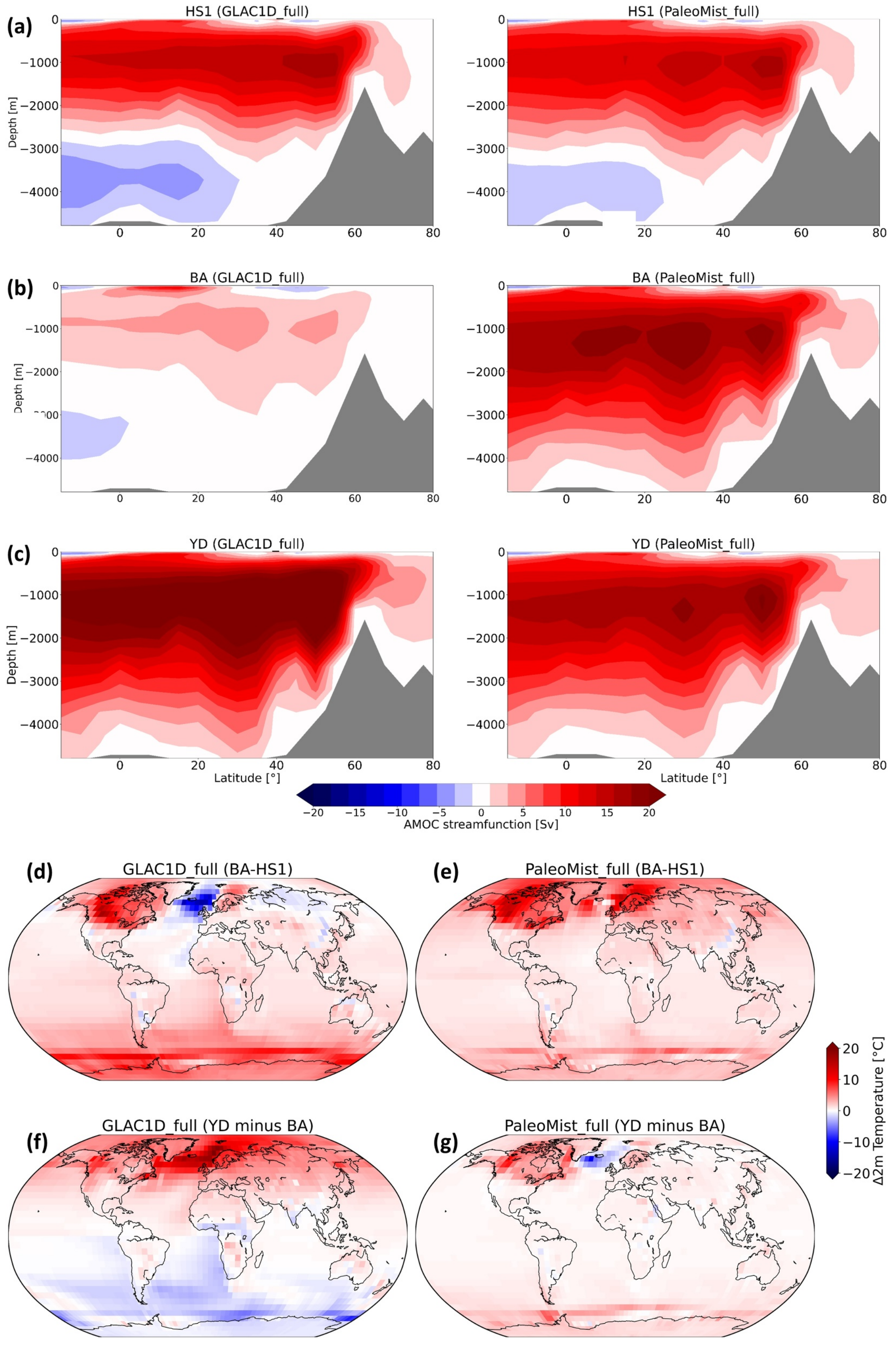


**Figure 3.** AMOC stream function for GLAC1D_full and PaleoMist_full during HS1, BA, and YD (a), (c), and (e). Near-surface temperature (2m temperature) anomalies between BA and HS1 and between YD and BA for PaleoMist_full (d) and (f) and GLAC1d_full (e) and (g), indicating the differences in the regional temperature signatures. The shown variables are averaged over the defined intervals.

Lohmann, 2003; Lohmann et al., 2020; Zhang et al., 2017). The exact timing of the BA/YD sequence with respect to Shakun et al. (2012) and data assimilation-based Osman et al. (2021) reconstructions is a subject of further investigation. Besides model uncertainties, we cannot exclude dating uncertainties of marine sediment cores due to changes in reservoir ages (e.g., Butzin et al., 2017; Lohmann et al., 2020).

Assessing the contributions of ice sheets, GHGs, and orbital forcing to warming during the last deglaciation, we demonstrate the significant role played by both GHGs and orbital forcing in regulating the freshwater flux into the North Atlantic, consequently affecting SSS and ocean circulation, consistent with (e.g., Bethke et al., 2012; He, 2011). The timing of deglacial transitions is particularly influenced by the magnitude of freshwater fluxes associated with the retreat of Northern Hemisphere ice sheets (Ganopolski & Roche, 2009; Knorr & Lohmann, 2003, 2007). As an extreme case, Liu et al. (2009) proposed that BA warming is controlled by the cessation of freshwater input, highlighting the significant role of deglacial freshwater in the abrupt recovery of AMOC. However, this freshwater history would be inconsistent with paleo-sea level proxies and both ice sheet reconstructions used here. We indicate that GHGs and orbital forcing influence the precipitation patterns, affecting the proximity of the AMOC to its bifurcation point between the on- and off-mode states. A significant reduction in freshwater input can lead to a shift in AMOC to a more stable mode. Our experiments could be further developed as a way to better assess the history of ice sheet evolution. Climate-ice sheet models combined with data assimilation could be suitable for estimating the ice sheets and deglacial meltwater.

The dynamics of the last termination include a reduction in the height of the ice sheets and an increase in GHG concentrations to achieve appropriate warming. The direct effect of orbital forcing on global mean surface temperature is relatively small. This will be different in a fully interactive Earth system model including ice sheets (e.g., Ganopolski & Brovkin, 2017; Willeit et al., 2019), then the glacial termination is triggered by orbital forcing. Simulations with prescribed ice sheets cannot resemble the full dynamics of the termination as in such simulations, the deglacial freshwater flux acts as a forcing rather than a response to AMOC changes (Lohmann & Schulz, 2000). As a logical next step, transient simulation of the last deglaciation with fully interactive ice sheets will explore the climate and biogeochemical feedback in the system. Single forcing experiments are deemed to be important in evaluating the phase-space and instabilities in the system.

## Data Availability Statement

The source code of CLIMBER-X (Version V2) and the instructions to install and run the model are available through Willeit et al. (2022). The output of simulations used for the analysis and figures is archived on Zenodo (https://doi.org/10.5281/zenodo.10159104, Masoum, 2023).

**Acknowledgments**
The authors wish to thank the AWI computing center for their help. Thanks to Evan J. Gowan for advising on PaleoMist ice sheet reconstruction. We acknowledge support by the Open Access publication fund of Alfred-Wegener-Institut (AWI) Helmholtz-Zentrum für Polar- und Meeresforschung. Ahmadreza Masoum and Gerrit Lohmann receive funding through Center for Marine Environmental Sciences at the University of Bremen (https://www.marum.de/en/Research/MARUM-Cluster-of-Excellence-Projects-OC.html), "Ocean and Cryosphere under climate change" in the Program "Changing Earth Sustaining our Future" of the Helmholtz Society (https://www.helmholtz.de/en/about-us/structure-and-governance/program-oriented-funding/) and through PalMod by the Bundesministerium für Bildung und Forschung (https://www.palmod.de/; Grant 01LP1917A). The funders had no role in study design, data collection and analysis, decision to publish, or preparation of the manuscript. Open Access funding enabled and organized by Projekt DEAL.

## References

Abe-Ouchi, A., Saito, F., Kawamura, K., Raymo, M. E., Okuno, J., Takahashi, K., & Blatter, H. (2013). Insolation-driven 100,000-year glacial cycles and hysteresis of ice-sheet volume. *Nature*, *500*(7461), 190–193. https://doi.org/10.1038/nature12374

Annan, J. D., Hargreaves, J. C., & Mauritsen, T. (2022). A new global surface temperature reconstruction for the last glacial maximum. *Climate of the Past*, *18*(8), 1883–1896. https://doi.org/10.5194/cp-18-1883-2022

Argus, D. F., Peltier, W., Drummond, R., & Moore, A. W. (2014). The antarctica component of postglacial rebound model ice-6g_c (vm5a) based on gps positioning, exposure age dating of ice thicknesses, and relative sea level histories. *Geophysical Journal International*, *198*(1), 537–563. https://doi.org/10.1093/gji/ggu140

Bakker, P., Rogozhina, I., Merkel, U., & Prange, M. (2020). Hypersensitivity of glacial summer temperatures in siberia. *Climate of the Past*, *16*(1), 371–386. https://doi.org/10.5194/cp-16-371-2020

Bethke, I., Li, C., & Nisancioglu, K. H. (2012). Can we use ice sheet reconstructions to constrain meltwater for deglacial simulations? *Paleoceanography*, *27*(2). https://doi.org/10.1029/2011pa002258

Bonelli, S., Charbit, S., Kageyama, M., Woillez, M.-N., Ramstein, G., Dumas, C., & Quiquet, A. (2009). Investigating the evolution of major northern hemisphere ice sheets during the last glacial-interglacial cycle. *Climate of the Past*, *5*(3), 329–345. https://doi.org/10.5194/cp-5-329-2009

Bouttes, N., Lhardy, F., Quiquet, A., Paillard, D., Goosse, H., & Roche, D. M. (2023). Deglacial climate changes as forced by different ice sheet reconstructions. *Climate of the Past*, *19*(5), 1027–1042. https://doi.org/10.5194/cp-19-1027-2023

Briggs, R. D., Pollard, D., & Tarasov, L. (2014). A data-constrained large ensemble analysis of antarctic evolution since the eemian. *Quaternary Science Reviews*, *103*, 91–115. https://doi.org/10.1016/j.quascirev.2014.09.003

Broecker, W. S. (2002). *The glacial world according to wally*. Lamont-Doherty earth observatory of Columbia University.

Buizert, C., Gkinis, V., Severinghaus, J. P., He, F., Lecavalier, B. S., Kindler, P., et al., (2014). Greenland temperature response to climate forcing during the last deglaciation. *Science*, *345*(6201), 1177–1180. https://doi.org/10.1126/science.1254961

Butzin, M., Köhler, P., & Lohmann, G. (2017). Marine radiocarbon reservoir age simulations for the past 50,000 years. *Geophysical Research Letters*, *44*(16), 8473–8480. https://doi.org/10.1002/2017gl074688

Carlson, A. E., Clark, P. U., Haley, B. A., Klinkhammer, G. P., Simmons, K., Brook, E. J., & Meissner, K. J. (2007). Geochemical proxies of north american freshwater routing during the younger dryas cold event. *Proceedings of the National Academy of Sciences*, *104*(16), 6556–6561. https://doi.org/10.1073/pnas.0611313104

Charbit, S., Kageyama, M., Roche, D., Ritz, C., & Ramstein, G. (2005). Investigating the mechanisms leading to the deglaciation of past continental northern hemisphere ice sheets with the climber–gremlins coupled model. *Global and Planetary Change*, *48*(4), 253–273. https://doi.org/10.1016/j.gloplacha.2005.01.002

Clark, P. U., Pisias, N. G., Stocker, T. F., & Weaver, A. J. (2002). The role of the thermohaline circulation in abrupt climate change. *Nature*, *415*(6874), 863–869. https://doi.org/10.1038/415863a

Clark, P. U., Shakun, J. D., Baker, P. A., Bartlein, P. J., Brewer, S., Brook, E., et al., (2012). Global climate evolution during the last deglaciation. *Proceedings of the National Academy of Sciences*, *109*(19), E1134–E1142. https://doi.org/10.1073/pnas.1116619109

Clark, P. U., & Tarasov, L. (2014). Closing the sea level budget at the last glacial maximum. *Proceedings of the National Academy of Sciences*, *111*(45), 15861–15862. https://doi.org/10.1073/pnas.1418970111

Claussen, M., Mysak, L., Weaver, A., Crucifix, M., Fichefet, T., & Loutre, M.-F., (2002). Earth system models of intermediate complexity: Closing the gap in the spectrum of climate system models. *Climate Dynamics*, *18*(7), 579–586. https://doi.org/10.1007/s00382-001-0200-1

Edwards, N., & Shepherd, J. (2002). Bifurcations of the thermohaline circulation in a simplified three-dimensional model of the world ocean and the effects of inter-basin connectivity. *Climate Dynamics*, *19*(1), 31–42. https://doi.org/10.1007/s00382-001-0207-7

Edwards, N. R., & Marsh, R. (2005). Uncertainties due to transport-parameter sensitivity in an efficient 3-d ocean-climate model. *Climate Dynamics*, *24*(4), 415–433. https://doi.org/10.1007/s00382-004-0508-8

Edwards, N. R., Willmott, A. J., & Killworth, P. D. (1998). On the role of topography and wind stress on the stability of the thermohaline circulation. *Journal of Physical Oceanography*, *28*(5), 756–778. https://doi.org/10.1175/1520-0485(1998)028<0756:otrota>2.0.co;2

Ganopolski, A., & Brovkin, V. (2017). Simulation of climate, ice sheets and co 2 evolution during the last four glacial cycles with an earth system model of intermediate complexity. *Climate of the Past*, *13*(12), 1695–1716. https://doi.org/10.5194/cp-13-1695-2017

Ganopolski, A., & Calov, R. (2011). The role of orbital forcing, carbon dioxide and regolith in 100 kyr glacial cycles. *Climate of the Past*, *7*(4), 1415–1425. https://doi.org/10.5194/cp-7-1415-2011

Ganopolski, A., & Roche, D. M. (2009). On the nature of lead–lag relationships during glacial–interglacial climate transitions. *Quaternary Science Reviews*, *28*(27–28), 3361–3378. https://doi.org/10.1016/j.quascirev.2009.09.019

Gowan, E. J., Tregoning, P., Purcell, A., Lea, J., Fransner, O. J., Noormets, R., & Dowdeswell, J. (2016). Icesheet 1.0: A program to produce paleo-ice sheet reconstructions with minimal assumptions. *Geoscientific Model Development*, *9*(5), 1673–1682. https://doi.org/10.5194/gmd-9-1673-2016

Gowan, E. J., Zhang, X., Khosravi, S., Rovere, A., Stocchi, P., Hughes, A. L., et al. (2021). A new global ice sheet reconstruction for the past 80 000 years. *Nature Communications*, *12*(1), 1–9. https://doi.org/10.1038/s41467-021-21469-w

Gowan, E. J., Zhang, X., Khosravi, S., Rovere, A., Stocchi, P., Hughes, A. L., et al. (2022). Reply to: Towards solving the missing ice problem and the importance of rigorous model data comparisons. *Nature Communications*, *13*(1), 6264. https://doi.org/10.1038/s41467-022-33954-x

Gregoire, L. J., Valdes, P. J., & Payne, A. J. (2015). The relative contribution of orbital forcing and greenhouse gases to the north american deglaciation. *Geophysical Research Letters*, *42*(22), 9970–9979. https://doi.org/10.1002/2015gl066005

He, F. (2011). Simulating transient climate evolution of the last deglaciation with ccsm 3 (Vol. *72*) (No. 10).

Heinemann, M., Timmermann, A., Elison Timm, O., Saito, F., & Abe-Ouchi, A. (2014). Deglacial ice sheet meltdown: Orbital pacemaking and co 2 effects. *Climate of the Past*, *10*(4), 1567–1579. https://doi.org/10.5194/cp-10-1567-2014

Held, H., & Kleinen, T. (2004). Detection of climate system bifurcations by degenerate fingerprinting. *Geophysical Research Letters*, *31*(23). https://doi.org/10.1029/2004gl020972

Ivanovic, R. F., Gregoire, L. J., Kageyama, M., Roche, D. M., Valdes, P. J., Burke, A., et al. (2016). Transient climate simulations of the deglaciation 21–9 thousand years before present (version 1)–pmip4 core experiment design and boundary conditions. *Geoscientific Model Development*, *9*(7), 2563–2587. https://doi.org/10.5194/gmd-9-2563-2016

Kageyama, M., Albani, S., Braconnot, P., Harrison, S. P., Hopcroft, P. O., Ivanovic, R. F., et al., (2017). The PMIP4 contribution to CMIP6–Part 4: Scientific objectives and experimental design of the PMIP4-CMIP6 last glacial maximum experiments and PMIP4 sensitivity experiments. *Geoscientific Model Development*, *10*(11), 4035–4055. https://doi.org/10.5194/gmd-10-4035-2017

Kageyama, M., Paul, A., Roche, D. M., & Van Meerbeeck, C. J. (2010). Modelling glacial climatic millennial-scale variability related to changes in the atlantic meridional overturning circulation: A review. *Quaternary Science Reviews*, *29*(21–22), 2931–2956. https://doi.org/10.1016/j.quascirev.2010.05.029

Kageyama, M., & Valdes, P. J. (2000). Impact of the north american ice-sheet orography on the last glacial maximum eddies and snowfall. *Geophysical Research Letters*, *27*(10), 1515–1518. https://doi.org/10.1029/1999gl011274

Kapsch, M.-L., Mikolajewicz, U., Ziemen, F., & Schannwell, C. (2022). Ocean response in transient simulations of the last deglaciation dominated by underlying ice-sheet reconstruction and method of meltwater distribution. *Geophysical Research Letters*, *49*(3), e2021GL096767. https://doi.org/10.1029/2021gl096767

Klockmann, M., Mikolajewicz, U., & Marotzke, J. (2018). Two amoc states in response to decreasing greenhouse gas concentrations in the coupled climate model mpi-esm. *Journal of Climate*, *31*(19), 7969–7984. https://doi.org/10.1175/jcli-d-17-0859.1

Knorr, G., & Lohmann, G. (2003). Southern ocean origin for the resumption of atlantic thermohaline circulation during deglaciation. *Nature*, *424*(6948), 532–536. https://doi.org/10.1038/nature01855

Knorr, G., & Lohmann, G. (2007). Rapid transitions in the atlantic thermohaline circulation triggered by global warming and meltwater during the last deglaciation. *Geochemistry, Geophysics, Geosystems*, *8*(12). https://doi.org/10.1029/2007gc001604

Köhler, P., Nehrbass-Ahles, C., Schmitt, J., Stocker, T. F., & Fischer, H. (2017). A 156 kyr smoothed history of the atmospheric greenhouse gases co 2, ch 4, and n 2 o and their radiative forcing. *Earth System Science Data*, *9*(1), 363–387. https://doi.org/10.5194/essd-9-363-2017

Lambeck, K., Rouby, H., Purcell, A., Sun, Y., & Sambridge, M. (2014). Sea level and global ice volumes from the last glacial maximum to the holocene. *Proceedings of the National Academy of Sciences*, *111*(43), 15296–15303. https://doi.org/10.1073/pnas.1411762111

Laskar, J., Robutel, P., Joutel, F., Gastineau, M., Correia, A., & Levrard, B. (2004). A long-term numerical solution for the insolation quantities of the earth. *Astronomy and Astrophysics*, *428*(1), 261–285. https://doi.org/10.1051/0004-6361:20041335

Liu, Z., Otto-Bliesner, B., He, F., Brady, E., Tomas, R., Clark, P., et al., (2009). Transient simulation of last deglaciation with a new mechanism for bølling-allerød warming. *Science*, *325*(5938), 310–314. https://doi.org/10.1126/science.1171041

Liu, Z., Zhu, J., Rosenthal, Y., Zhang, X., Otto-Bliesner, B. L., Timmermann, A., et al. (2014). The holocene temperature conundrum. *Proceedings of the National Academy of Sciences*, *111*(34), E3501–E3505. https://doi.org/10.1073/pnas.1407229111

Löfverström, M., Caballero, R., Nilsson, J., & Kleman, J. (2014). Evolution of the large-scale atmospheric circulation in response to changing ice sheets over the last glacial cycle. *Climate of the Past*, *10*(4), 1453–1471. https://doi.org/10.5194/cp-10-1453-2014

Löfverström, M., & Lora, J. M. (2017). Abrupt regime shifts in the north atlantic atmospheric circulation over the last deglaciation. *Geophysical Research Letters*, *44*(15), 8047–8055. https://doi.org/10.1002/2017gl074274

Lohmann, G., Butzin, M., Eissner, N., Shi, X., & Stepanek, C. (2020). Abrupt climate and weather changes across time scales. *Paleoceanography and Paleoclimatology*, *35*(9), e2019PA003782. https://doi.org/10.1029/2019pa003782

Lohmann, G., & Schneider, J. (1999). Dynamics and predictability of stommel's box model. a phase-space perspective with implications for decadal climate variability. *Tellus*, *51*(2), 326–336. https://doi.org/10.3402/tellusa.v51i2.12314

Lohmann, G., & Schulz, M. (2000). Reconciling bølling warmth with peak deglacial meltwater discharge. *Paleoceanography*, *15*(5), 537–540. https://doi.org/10.1029/1999pa000471

Marcott, S. A., Shakun, J. D., Clark, P. U., & Mix, A. C. (2013). A reconstruction of regional and global temperature for the past 11,300 years. *Science*, *339*(6124), 1198–1201. https://doi.org/10.1126/science.1228026

MARGO. (2009). Constraints on the magnitude and patterns of ocean cooling at the last glacial maximum. *Nature Geoscience*, *2*(2), 127–132. https://doi.org/10.1038/ngeo411

Masoum, A. (2023). Evaluating forcing factors of the last deglaciation: Lessons from an efficient earth system model. [dataset]. https://doi.org/10.5281/zenodo.10159104

McManus, J. F., Francois, R., Gherardi, J.-M., Keigwin, L. D., & Brown-Leger, S. (2004). Collapse and rapid resumption of atlantic meridional circulation linked to deglacial climate changes. *Nature*, *428*(6985), 834–837. https://doi.org/10.1038/nature02494

Monnin, E., Indermuhle, A., Dallenbach, A., Fluckiger, J., Stauffer, B., Stocker, T. F., et al. (2001). Atmospheric CO2 concentrations over the last glacial termination. *Science*, *291*(5501), 112–114. https://doi.org/10.1126/science.291.5501.112

Ng, H. C., Robinson, L. F., McManus, J. F., Mohamed, K. J., Jacobel, A. W., Ivanovic, R. F., et al. (2018). Coherent deglacial changes in western atlantic ocean circulation. *Nature Communications*, *9*(1), 2947. https://doi.org/10.1038/s41467-018-05312-3

Obase, T., & Abe-Ouchi, A. (2019). Abrupt bølling-allerød warming simulated under gradual forcing of the last deglaciation. *Geophysical Research Letters*, *46*(20), 11397–11405. https://doi.org/10.1029/2019gl084675

Osman, M. B., Tierney, J. E., Zhu, J., Tardif, R., Hakim, G. J., King, J., & Poulsen, C. J. (2021). Globally resolved surface temperatures since the last glacial maximum. *Nature*, *599*(7884), 239–244. https://doi.org/10.1038/s41586-021-03984-4

Paillard, D. (2015). Quaternary glaciations: From observations to theories. *Quaternary Science Reviews*, *107*, 11–24. https://doi.org/10.1016/j.quascirev.2014.10.002

Peltier, W. (2005). On the hemispheric origins of meltwater pulse 1A. *Quaternary Science Reviews*, *24*(14–15), 1655–1671. https://doi.org/10.1016/j.quascirev.2004.06.023

Peltier, W. R. (1994). Ice age paleotopography. *Science*, *265*(5169), 195–201. https://doi.org/10.1126/science.265.5169.195

Peltier, W. R. (2004). Global glacial isostasy and the surface of the ice-age earth: The ice-5g (vm2) model and grace. *Annual Review of Earth and Planetary Sciences*, *32*(1), 111–149. https://doi.org/10.1146/annurev.earth.32.082503.144359

Peltier, W. R., Argus, D., & Drummond, R. (2015). Space geodesy constrains ice age terminal deglaciation: The global ice-6g_c (vm5a) model. *Journal of Geophysical Research: Solid Earth*, *120*(1), 450–487. https://doi.org/10.1002/2014jb011176

Pöppelmeier, F., Jeltsch-Thömmes, A., Lippold, J., Joos, F., & Stocker, T. F. (2023). Multi-proxy constraints on atlantic circulation dynamics since the last ice age. *Nature Geoscience*, *16*(4), 349–356. https://doi.org/10.1038/s41561-023-01140-3

Roche, D. M., Wiersma, A. P., & Renssen, H. (2010). A systematic study of the impact of freshwater pulses with respect to different geographical locations. *Climate Dynamics*, *34*(7–8), 997–1013. https://doi.org/10.1007/s00382-009-0578-8

Shakun, J. D., Clark, P. U., He, F., Marcott, S. A., Mix, A. C., Liu, Z., et al. (2012). Global warming preceded by increasing carbon dioxide concentrations during the last deglaciation. *Nature*, *484*(7392), 49–54. https://doi.org/10.1038/nature10915

Sherriff-Tadano, S., Abe-Ouchi, A., Yoshimori, M., Oka, A., & Chan, W.-L. (2018). Influence of glacial ice sheets on the atlantic meridional overturning circulation through surface wind change. *Climate Dynamics*, *50*(7–8), 2881–2903. https://doi.org/10.1007/s00382-017-3780-0

Smith, R. S., & Gregory, J. M. (2009). A study of the sensitivity of ocean overturning circulation and climate to freshwater input in different regions of the north atlantic. *Geophysical Research Letters*, *36*(15). https://doi.org/10.1029/2009gl038607

Snoll, B., Ivanovic, R., Gregoire, L., Sherriff-Tadano, S., Menviel, L., Obase, T., et al., (2024). A multi-model assessment of the early last deglaciation (pmip4 ldv1): A meltwater perspective. *Climate of the Past*, *20*(4), 789–815. https://doi.org/10.5194/cp-20-789-2024

Spada, G., & Stocchi, P. (2007). Selen: A fortran 90 program for solving the "sea-level equation". *Computers and Geosciences*, *33*(4), 538–562. https://doi.org/10.1016/j.cageo.2006.08.006

Spahni, R., Chappellaz, J., Stocker, T. F., Loulergue, L., Hausammann, G., Kawamura, K., et al., (2005). Atmospheric methane and nitrous oxide of the late pleistocene from antarctic ice cores. *Science*, *310*(5752), 1317–1321. https://doi.org/10.1126/science.1120132

Stouffer, R. J., Seidov, D., & Haupt, B. J. (2007). Climate response to external sources of freshwater: North atlantic versus the southern ocean. *Journal of Climate*, *20*(3), 436–448. https://doi.org/10.1175/jcli4015.1

Stouffer, R. J., Yin, J., Gregory, J., Dixon, K., Spelman, M., Hurlin, W., et al., (2006). Investigating the causes of the response of the thermohaline circulation to past and future climate changes. *Journal of Climate*, *19*(8), 1365–1387. https://doi.org/10.1175/jcli3689.1

Sun, Y., Knorr, G., Zhang, X., Tarasov, L., Barker, S., Werner, M., & Lohmann, G. (2022). Ice sheet decline and rising atmospheric CO2 control amoc sensitivity to deglacial meltwater discharge. *Global and Planetary Change*, *210*, 103755. https://doi.org/10.1016/j.gloplacha.2022.103755

Tarasov, L., Dyke, A. S., Neal, R. M., & Peltier, W. R. (2012). A data-calibrated distribution of deglacial chronologies for the north american ice complex from glaciological modeling. *Earth and Planetary Science Letters*, *315*, 30–40. https://doi.org/10.1016/j.epsl.2011.09.010

Tarasov, L., & Richard Peltier, W. (2002). Greenland glacial history and local geodynamic consequences. *Geophysical Journal International*, *150*(1), 198–229. https://doi.org/10.1046/j.1365-246x.2002.01702.x

Tierney, J. E., Zhu, J., King, J., Malevich, S. B., Hakim, G. J., & Poulsen, C. J. (2020). Glacial cooling and climate sensitivity revisited. *Nature*, *584*(7822), 569–573. https://doi.org/10.1038/s41586-020-2617-x

Timmermann, A., Timm, O., Stott, L., & Menviel, L. (2009). The roles of co2 and orbital forcing in driving southern hemispheric temperature variations during the last 21 000 yr. *Journal of Climate*, *22*(7), 1626–1640. https://doi.org/10.1175/2008jcli2161.1

Ullman, D., LeGrande, A., Carlson, A. E., Anslow, F., & Licciardi, J. (2014). Assessing the impact of laurentide ice sheet topography on glacial climate. *Climate of the Past*, *10*(2), 487–507. https://doi.org/10.5194/cp-10-487-2014

Veres, D., Bazin, L., Landais, A., Toyé Mahamadou Kele, H., Lemieux-Dudon, B., Parrenin, F., et al., (2013). The antarctic ice core chronology (aicc2012): An optimized multi-parameter and multi-site dating approach for the last 120 thousand years. *Climate of the Past*, *9*(4), 1733–1748. https://doi.org/10.5194/cp-9-1733-2013

Waelbroeck, C., Duplessy, J.-C., Michel, E., Labeyrie, L., Paillard, D., & Duprat, J. (2001). The timing of the last deglaciation in north atlantic climate records. *Nature*, *412*(6848), 724–727. https://doi.org/10.1038/35089060

Weaver, A. J., Saenko, O. A., Clark, P. U., & Mitrovica, J. X. (2003). Meltwater pulse 1a from Antarctica as a trigger of the bølling-allerød warm interval. *Science*, *299*(5613), 1709–1713. https://doi.org/10.1126/science.1081002

Willeit, M., & Ganopolski, A. (2016). Paladyn v1. 0, a comprehensive land surface–vegetation–carbon cycle model of intermediate complexity. *Geoscientific Model Development*, *9*(10), 3817–3857. https://doi.org/10.5194/gmd-9-3817-2016

Willeit, M., Ganopolski, A., Calov, R., & Brovkin, V. (2019). Mid-pleistocene transition in glacial cycles explained by declining co2 and regolith removal. *Science Advances*, *5*(4), eaav7337. https://doi.org/10.1126/sciadv.aav7337

Willeit, M., Ganopolski, A., Robinson, A., & Edwards, N. R. (2022). The earth system model climber-x v1. 0–part 1: Climate model description and validation. *Geoscientific Model Development*, *15*(14), 5905–5948. https://doi.org/10.5194/gmd-15-5905-2022

Yokoyama, Y., Lambeck, K., De Deckker, P., Esat, T. M., Webster, J. M., & Nakada, M. (2022). Towards solving the missing ice problem and the importance of rigorous model data comparisons. *Nature Communications*, *13*(1), 6261. https://doi.org/10.1038/s41467-022-33952-z

Zhang, X., Barker, S., Knorr, G., Lohmann, G., Drysdale, R., Sun, Y., et al. (2021). Direct astronomical influence on abrupt climate variability. *Nature Geoscience*, *14*(11), 819–826. https://doi.org/10.1038/s41561-021-00846-6

Zhang, X., Knorr, G., Lohmann, G., & Barker, S. (2017). Abrupt north atlantic circulation changes in response to gradual CO2 forcing in a glacial climate state. *Nature Geoscience*, *10*(7), 518–523. https://doi.org/10.1038/ngeo2974

Zhang, X., Lohmann, G., Knorr, G., & Purcell, C. (2014a). Abrupt glacial climate shifts controlled by ice sheet changes. *Nature*, *512*(7514), 290–294. https://doi.org/10.1038/nature13592

Zhang, X., Lohmann, G., Knorr, G., & Purcell, C. (2014b). Control of rapid glacial climate shifts by variations in intermediate ice-sheet volume. *Nature*, *512*(7514), 290–294. https://doi.org/10.1038/nature13592

Zhu, J., Liu, Z., Zhang, X., Eisenman, I., & Liu, W. (2014). Linear weakening of the amoc in response to receding glacial ice sheets in ccsm3. *Geophysical Research Letters*, *41*(17), 6252–6258. https://doi.org/10.1002/2014gl060891